GA–A26123

PARTICLE, HEAT, AND SHEATH POWER TRANSMISSION FACTOR PROFILES DURING ELM SUPPRESSION EXPERIMENTS ON DIII-D

by
J.G. WATKINS, T.E. EVANS, I. JOSEPH, C.J. LASNIER, R.A. MOYER,
D.L. RUDAKOV, O. SCHMITZ, M. JAKUBOWSKI,
and M.E. FENSTERMACHER

JUNE 2008

GENERAL ATOMICS

DISCLAIMER

GA–A26123

PARTICLE, HEAT, AND SHEATH POWER TRANSMISSION FACTOR PROFILES DURING ELM SUPPRESSION EXPERIMENTS ON DIII-D

by
J.G. WATKINS,* T.E. EVANS, I. JOSEPH,† C.J. LASNIER,† R.A. MOYER,‡
D.L. RUDAKOV,‡ O. SCHMITZ,§ M. JAKUBOWSKI,£
and M.E. FENSTERMACHER†

This is a preprint of a paper to be presented at the Eighteenth International Conference on Plasma Surface Interactions, May 26-30, 2008, in Toledo, Spain, and to be published in the *J. Nucl. Mater.*

*Sandia National Laboratories, Albuquerque, New Mexico
†Lawrence Livermore National Laboratory, Livermore, California
‡University of California-San Diego, La Jolla, California
§Forschungzentrum-Jülich, IEF4 – Plasmaphysik, Jülich, Germany
£Max- Planck-Institut für Plasmaphysik, Greifswald, Germany

Work supported in part by
the U.S. Department of Energy
under DE-AC04-94AL85000, DE-FC02-04ER54698,
DE-AC52-07NA27344, and DE-FG02-07ER54917

GENERAL ATOMICS ATOMICS PROJECT 30200
JUNE 2008

GENERAL ATOMICS

ABSTRACT

Edge localized modes (ELMs) are predicted to be a significant problem for ITER due to impulse heating of the divertor target plates. During low collisionality experiments on DIII-D where ELMs were suppressed using resonant magnetic perturbations (RMP), target plate profiles of particle flux (J_{sat}), electron temperature (T_e), and floating potential (V_f) have been measured with Langmuir probes (LP) and compared to IRTV heat flux profiles. During ELM suppression, J_{sat} and T_e increase and the J_{sat} profile broadens. A three-peak structure, most visible in the V_f, agrees with the spacing and q_{95} dependence of an $n = 3$ toroidal pattern predicted by the TRIP3D code. The heat flux calculated from Langmuir probe data (using sheath theory) is observed to get approximately 2x larger during ELM suppression than between ELMs before the RMP is turned on. The sheath power transmission factor profile has been determined from IRTV and Langmuir probe data.

I. INTRODUCTION

Edge localized modes (ELMs) are predicted to be a problem for ITER due to resulting high levels of impulse heating and erosion of the target plates [1,2]. Using a resonant magnetic perturbation (RMP), ELMs have been suppressed in DIII-D [3]. But what happens to the heat and particle flux at the target plate under these conditions? Is there any evidence of the RMP on the target plate? Measurements under these conditions have been reported previously [4] at one point in the target plate scrape-off layer (SOL). In this paper, we report the first observations of the target plate plasma profiles measured by Langmuir probes (LP) [5] during ELM suppression and compare these profiles using sheath theory with IR camera heat flux measurements and predictions of the field line tracing code TRIP3D. The sheath power transmission factor, γ, which relates particle flux to heat flux (i.e. $q = \gamma \Gamma T_e$, where q is the heat flux and $\Gamma = n_e C_s = J_{sat}/e$ is the particle flux), is determined from these measurements to investigate if the data departs from normal sheath theory (i.e. if evidence of fast, non-Maxwellian particles can be detected at the divertor plates).

II. OBSERVATIONS

The plasma discharges are similar to those described in Ref. [3] and are low pedestal collisionality, high confinement, pumped, unbalanced double null shapes scaled down from one of the ITER shapes. Even though the divertor cryopumps were on for the entire shot, the core density only decreases significantly after the RMP is applied. The target plate profiles shown in this paper are measured at the outer divertor target plate strike point using strike point sweeps (1) before the RMP is applied (ELMing) and (2) well after the density decreases and the ELMs are suppressed.

ELM suppression produces significant changes at the target plate as shown in Fig. 1. For this case, the outer midplane/target plate flux expansion is 5.4. The spatial resolution of the profiles is significantly improved (probe width = 4 mm) through the use of strike point sweeps. We observe that the J_{sat} profile [Fig. 1(a)] increases and broadens during ELM suppression and the electron temperature profile [Fig. 1(b)] shows a significant (~100%) increase. The V_f profiles [Fig. 1(c)] show several large negative peaks and the calculated LP perpendicular heat flux profile [Fig. 1(d)] increases by about a factor of 2 and becomes broader. The heat flux in this figure is perpendicular to the tile surface using a constant factor $\gamma = 7$ based on standard sheath theory [6]. Based on the target plate profiles and core density pumpout [3], it appears that the core plasma radial transport increases with the RMP on (especially at resonant edge q) and allows the pumps to effectively exhaust particles and reduce both core density and recycling in the divertor. The reduced radiation in the divertor allows more heat flux to reach the divertor plates. . In addition to the increased heat flux from the reduced radiation, there may be an additional heat flux contribution from fast particles pulled out of the core plasma due to the magnetic perturbation.

The V_f radial profile clearly shows several negative peaks consistent (see below) with an $n = 3$ magnetic perturbation (RMP). The outermost structure observed in the radial V_f profile (Fig. 2) moves outward (toward larger major radius) when the plasma edge q increases slightly. The most negative V_f peak near the outer divertor strike point (i.e. the strike point from EFIT equilibrium reconstruction) does not change as the edge q changes.

In a different set of shots taken more recently, heat flux profile data is available from a fast framing IR camera. The camera profiles were acquired in full frame mode at 1.13 kHz. Using IR camera data acquired during the strike point sweeps, we have shifted each target plate IR profile relative to the target plate strike point location (determined from EFIT), and combined the data to get a much higher resolution profile. Figure 3(a) shows a comparison of the resulting IR heat flux profile with calculated heat flux from the measured Langmuir probe particle flux and electron temperature profiles using a sheath power transmission factor of $\gamma = 7$ ($q = \gamma \Gamma T_e$). Although there is evidence from some of the LP data that a structure is present, the pattern location seems to be moving due to small changes in the q_{95} for these shots and is not readily visible on the time averaged profiles shown in Fig. 3(a).

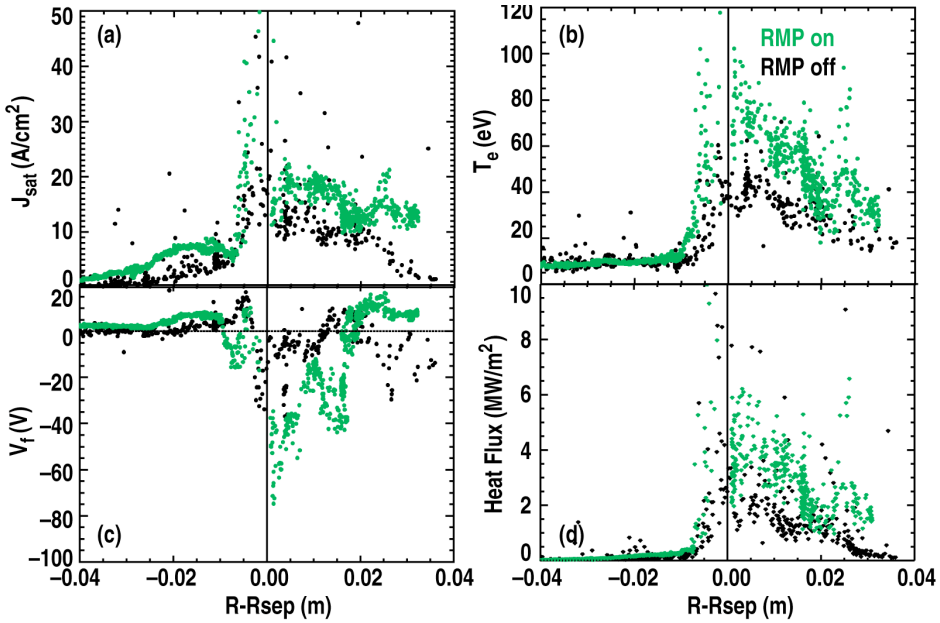

Fig. 1. Radial profiles during ELM suppression (green) of (a) J_{sat}, (b) electron temperature, (c) V_f, measured by Langmuir probes and (d) perpendicular heat flux calculated from (a) and (b) using a constant sheath factor of 7 across the entire profile (although the sheath factor is usually lower near the strike point). Also shown here are unperturbed profiles measured before the RMP coils were energized (black).

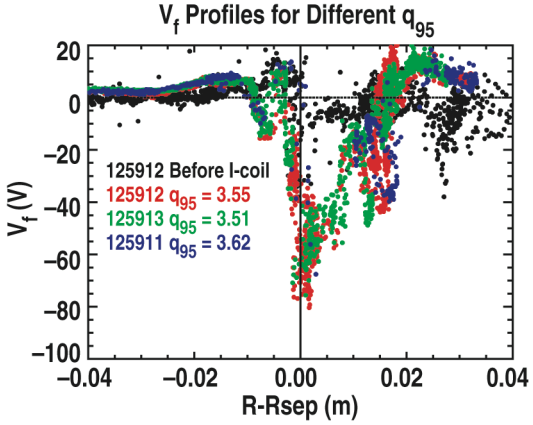

Fig. 2. V_f radial profiles measured during RMP ELM suppression for three different edge q values show evidence of a clockwise $n = 3$ pattern rotation as predicted by the TRIP3D code. A clockwise shift results in an outward radial shift in the profile at the LP location.

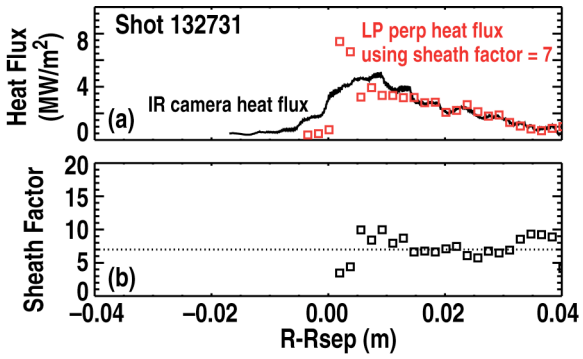

Fig. 3. (a) Heat flux profiles measured during ELM suppression from IR camera data and LP profiles (symbols) are compared using a constant value for the sheath factor (i.e., $\gamma = 7$). The LP measurement has been multiplied by the sine of the angle of the magnetic field with the tile surface for each probe location and time. The IR camera profile has been shifted out by 5 mm. (b) The measured sheath factor profile resulting from the IR and LP data shows a value of near 7 in the outer SOL and drops near the strike point similar to previous measurements in ELMing plasmas with no RMP.

III. DISCUSSION

When the ELM suppression coils are energized, the edge transport evidently increases based on the pump out of the core density. One would expect an increase in target plate electron temperature and V_f values due to the reduced core density (and therefore reduced divertor density). However, the onset of large negative V_f values is correlated with the rather sudden onset of ELM suppression [4] rather than the slower pump out observed when the RMP is energized. The sudden appearance of the V_f structure when ELMs were suppressed appears to be correlated with the onset of resonant conditions in the edge q and a minimum pedestal collisionality condition. This implies that the large negative V_f values are connected to the mechanism of ELM suppression and not just a result of reduced density.

The profile measurements indicate that the heat flux increase observed during ELM suppression results from both increased particle flux and increased electron temperature. These observations are consistent with an increase in transport of both particles and energy upstream of the divertor (i.e. convection or $E \times B$ radial transport).

Predictions of the target plate magnetic footprint using the TRIP3D code [7] (Fig. 4) show an $n = 3$ pattern. This code predicts where magnetic field lines launched just inside the separatrix escape the core plasma and impact the target plate. Magnetic field lines are followed to the target plate using the vacuum and equilibrium fields from an EFIT (toroidally symmetric) equilibrium plus the perturbation fields from the C-coils ($n = 1$, used for error field correction) and I-coils ($n = 3$, used for application of the RMP). The calculation results in an $n = 3$ spiral pattern toroidally around the divertor on the target plates, shown in Fig. 4, which appears to be similar to observed structures in the profiles at the location of the Langmuir probes. The edge q dependence of the target plate V_f structures is consistent with the TRIP3D predicted clockwise rotation (to the right in Fig. 4) of the spiral pattern in the toroidal direction with increased edge q. The magnetic footprint predicted near the strike point appears to be associated with the largest V_f negative peak and does not move radially with the q induced ($n = 3$) pattern rotation as we observe (Fig. 2).

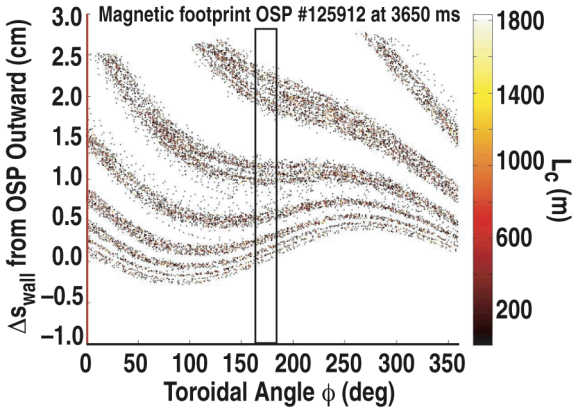

Fig. 4. This magnetic footprint shows the magnetic field line impact locations on the divertor plates for all of the core plasma field lines launched in the TRIP3D calculation. Colors (online) indicate the connection length from the launch point to the target plate. The vertical bar indicates the toroidal location of the Langmuir probes.

A more detailed comparison of the V_f radial profile using TRIP3D to follow target plate launched field lines (Fig. 5) reveals an interesting new interpretation of the V_f pattern. Here

field lines were launched from the divertor target plate every 0.5 mm and traced into the SOL or core plasma. The deepest penetration depth of about $\rho = 0.9$ (where $\rho = 1$ is the plasma boundary and $\rho = 0$ is the plasma center) correlates with the largest negative V_f value. Also, the width of the TRIP3D pattern is similar to the width of the pattern in the measured profile. The TRIP3D calculation indicates that the largest V_f peak should perhaps be interpreted as two peaks close together. The 4 mm wide probe tips radially average over the actual potential structure.

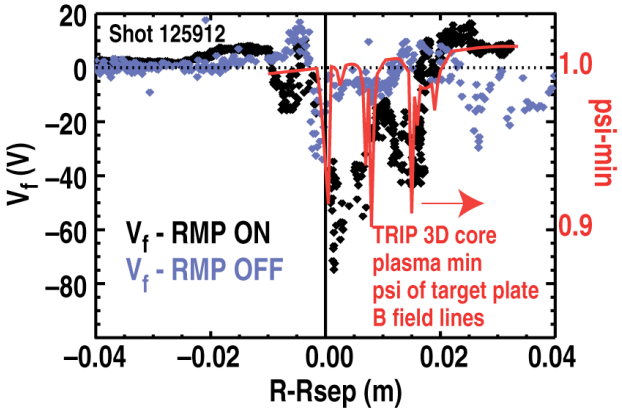

Fig. 5. Results from the TRIP3D code are compared to V_f radial profiles measured by the Langmuir probes during strike point sweeps. The TRIP3D calculated minimum psi (red – right scale) shows the innermost penetration of target plate field lines into the core plasma and the V_f radial profiles (left scale) are shown with the RMP on (black) and RMP off (blue). The field lines with the deepest penetration into the core plasma exhibit the most negative floating potentials at the target plate.

So it appears that during ELM suppression, the target plate V_f profile samples field lines that connect to the upstream pedestal conditions (inside the core plasma). Other experiments [8] have observed evidence of islands in the boundary plasma using V_f as an indicator. The fact that the V_f jump appears simultaneously with the ELM suppression indicates it is more closely related to the ELM-suppression mechanism rather than the application of the perturbation or the density pump-out. It appears to be necessary to cross some threshold in order for the suppression to take place. One such threshold condition could be the pedestal density or collisionality which allows thermal decoupling of the magnetic islands and onset of a high-m edge poloidal electric field structure, a potential “picket fence”, which would greatly enhance $E \times B$ radial transport. The other necessary condition is that the edge q resonance condition is satisfied to magnify the effect of the perturbation, increase the size of the islands, and pull core field lines out where they can hit the target plate. Field lines with longer connection length (from TRIP3D) come from deeper inside the core plasma and are also correlated with the V_f peak locations.

Island overlap has emerged as a useful criterion for ELM suppression to occur [9]. When this happens, the magnetic field lines surrounding pedestal magnetic islands becomes stochastic which may lead to even larger potential differences between the islands and the surrounding region. This effect would tend to enhance the poloidal electric field structure and boost radial $E \times B$ transport. This boost could provide the extra transport we need to suppress the ELMs.

One limitation of the measurements shown in Fig. 1 is that full ion saturation was not achieved for parts of the profile with the largest V_f values due to power supply limitations. The V_f and T_e profiles are unaffected by this limitation. Profiles used for the heat flux comparison shown in Fig. 3 are also affected by this problem near the strike point but the V_f levels were not as negative as in Fig. 2 and they did not clearly show the multi-peaked footprint as clearly either due to fluctuations in conditions (mostly edge q).

The heat flux profile calculated from the LP data (located at 180°) using a fixed sheath factor of 7 agrees fairly well with the measured IR camera profiles [Fig. 3(a)]. The IR camera profiles are measured at 165° and are from radial profiles taken in the middle of the floor tiles. The tile edges are very carefully aligned and edge heating effects have been greatly reduced but are still visible. The 2D heat transfer code, also used at TEXTOR [10] to convert IR camera surface temperature to heat flux, is the THEODOR code [11] with no surface layer. The outer strike point is a region of net erosion so deposited layers would not be an issue for these measurements. Based on the predicted magnetic footprint shown in Fig. 4, the two locations should be comparable. In Fig. 3(a), however, it was necessary to shift the IR heat flux profile (165 deg) by 5 mm toward larger major radius for the comparison with the LP profiles (180 deg) due to the $n = 1$ perturbation of the strike point seen in Fig. 4. The sheath factor profile shown in Fig. 3(b) is the factor needed to bring the IR and LP heat flux profiles into agreement at each location in the profile. This sheath factor profile does seem to exhibit the sheath factor drop ($\gamma \sim 1$) seen previously near the strike point [4] and does not look too different than previous measurements. We intend to repeat these measurements in the near future on ELM suppressed shots with better q_{95} control in hopes of resolving the sheath factor structure in more detail with a new IR camera now available on DIII-D.

IV. CONCLUSIONS

Target plate measurements in DIII-D indicate significant changes when ELMs are suppressed. Evidence of the $n = 3$ perturbation can be clearly observed as structures in the V_f radial profile and are consistent with TRIP3D predictions of target plate magnetic footprints and the rotation of these patterns with changing edge q. The potential structure seen on the target plate during ELM suppression indicates the onset of an upstream pedestal condition that connects field lines from the core plasma to the target plates, also predicted by TRIP3D. The steady state heat flux is higher and broader after ELMs are suppressed but implies better survivability for the ITER target plates due to the lack of impulse heating due to ELMs.

REFERENCES

[1] A.W. Leonard, *et al*., J. Nucl. Mater. **313-316** (2003) 768.

[2] A. Loarte, *et al*., Plasma Phys. Control. Fusion **45** (2003) 1549.

[3] T.E. Evans, *et al*., Phys. Rev. Lett. **92** (2004) 235003-1.

[4] J.G. Watkins, *et al.,* J. Nucl. Mater. **363** (2007) 708-712.

[5] J.G. Watkins, Rev. Sci. Instrum **79** (2008) 1

[6] P.C. Stangeby, *The Plasma Boundary of Magnetic Fusion Devices*, P. Stott and H. Wilhelmsson eds. (Inst. of Physics Publication, Taylor & Francis, 2000), p 92.

[7] T.E. Evans, R.A. Moyer and P. Monat, Phys. Plasmas **9** (2002) 4957.

[8] T.E. Evans, *et al*., J. Nucl. Mater. **162-164** (1989) 636-642.

[9] M.E. Fenstermacher, *et al.,* J. Nucl. Mater. **363** (2007) 476-483.

[10] M.W. Jakubowski. *et al*., Nuclear Fusion **44** (2004) S1-S11.

[11] A. Herrmann, *et al*., Plasma Physics and Controlled Fusion **37** (1995) 17-29.

ACKNOWLEDGMENT

This work was supported by the US Department of Energy under DE-AC04-94AL85000, DE-FC02-04ER54698, DE-AC52-07NA27344, and DE-FG02-07ER54917.